

Pushing Fast and Slow: Task-Adaptive MPC for Pushing Manipulation Under Uncertainty

Wisdom C. Agboh

Mehmet R. Dogar

Abstract—We propose a model predictive control approach to pushing based manipulation. The key feature of the algorithm is that it can adapt to the accuracy requirements of a task, by slowing down and generating “careful” motion when the task requires high accuracy, and by speeding up and moving fast when the task allows inaccuracy. We formulate the problem as an MDP and use an approximate online solution to the MDP. We use a trajectory optimizer with a deterministic model to suggest promising actions to the MDP, to reduce computation time spent on evaluating different actions. The trajectory optimizer is then initialized with trajectories with different speed profiles to generate a variety of actions for the MDP that can adapt to different tasks.

I. INTRODUCTION

We propose a model predictive control (MPC) algorithm for non-prehensile manipulation. The key feature of our algorithm is *task-adaptivity*: the controller can adapt to the accuracy requirements of a task, performing fast or slow pushes. For example in Fig. 1-top, the robot is pushing an object on a narrow strip. The task requires high-accuracy during pushing — otherwise the object can fall down. The controller therefore generates slow pushing actions that make small but careful progress to the goal pose of the object. In Fig. 1-bottom, however, the object is on a wide table and the goal region for the object is large (circle drawn on the table). In this case, the controller generates only a small number of fast pushing actions to reach the goal quickly — even if this creates more uncertainty about the object’s pose after each action, the task can still be completed successfully. We present a controller that can adapt to tasks with different accuracy requirements, such as in these examples.

There has been significant recent interest in non-prehensile pushing-based manipulation. Most existing work use motion planning and *open-loop* execution to address the problem of generating a sequence of actions to complete a non-prehensile manipulation task [8, 9, 3, 11, 6]. Others developed closed-loop approaches. Particularly, Hogan and Rodriguez [4] proposed a model predictive controller that uses integer programming to handle the different contact modes associated with the pusher-slider system. Arruda et al. [1] considered the task of pushing an object to a goal region while avoiding regions of high predictive uncertainty through model predictive path integral control. We take a similar approach and propose a closed-loop controller for pushing tasks.

A common feature of existing work is the reliance on the quasi-static model of pushing [10, 5]. While one reason of the popularity of the quasi-static model may be the simpler

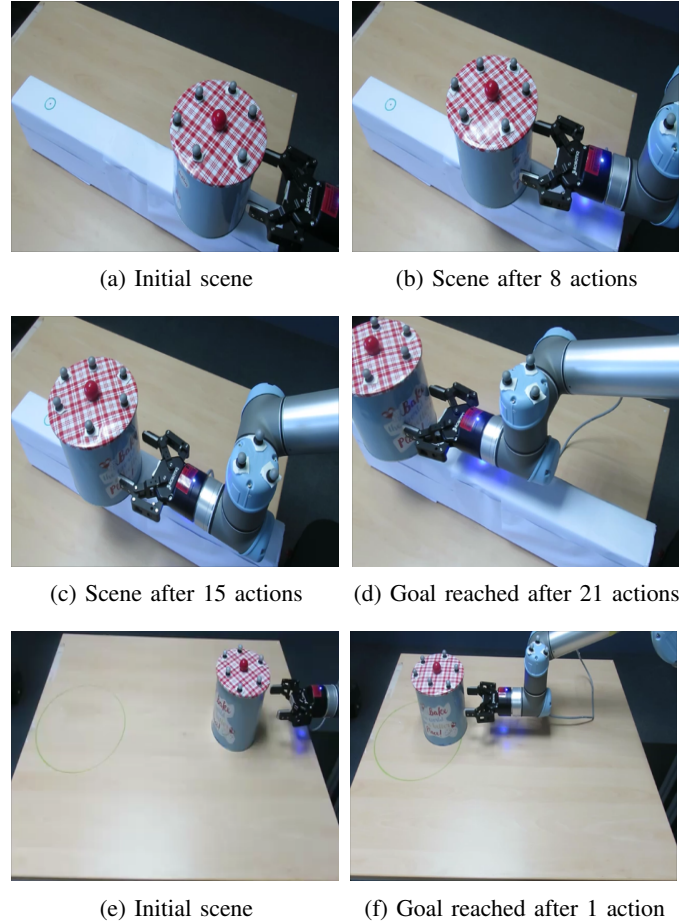


Fig. 1: Task-adaptive pushing with 21 slow actions for a high accuracy task (a-d) and a single fast action for a low accuracy task (e-f)

analytic equations of motion it enables one to derive, another reason is the slow nature of quasi-static interactions, which keeps the uncertainty during pushing tightly bounded and therefore easier to control accurately.

However, accuracy is not the main criterion for every task, as we illustrate in Fig. 1. Fast motions, even if inaccurate may be desired during some tasks. We humans also adapt our actions to the task. Imagine reaching into a fridge shelf that is crowded with fragile objects, such as glass jars and containers. You move slowly and carefully. However, if the fridge shelf is almost empty, only with a few plastic containers that are

difficult-to-break, you move faster with less care.

One way to build such a controller is to model the problem as a Markov Decision Process (MDP) with stochastic dynamics, where the stochasticity is action-dependent. Then, if this MDP is solved for an optimal policy under a cost that includes time to reach the goal, the resulting policy will use fast actions when it can, and fall back to slow actions for tasks that require higher accuracy.

In this paper, we model the problem as an MDP. However, we do not search for a globally optimal policy as this would be prohibitively computationally expensive. Instead, we solve the MDP online [12]. However, even in this online setting, evaluating the value of all possible actions (including actions of a wide variety of speeds), proves computationally expensive, since the cost of physics-based predictions are high. Therefore, instead of evaluating all possible actions, at any given state, we first use a fast trajectory optimizer to suggest a reduced set of promising actions, i.e. actions that are known to drive the system to the goal under the deterministic setting. We then evaluate these actions under stochasticity to pick the best one.

We make the following contributions:

- We propose a task-adaptive online solution to the stochastic MDP for pushing-based manipulation.
- We propose a trajectory optimizer to generate actions for evaluation under the MDP setting.
- We compare our task-adaptive method with a standard model predictive control approach using actions at the quasi-static speed. We show that our approach achieves similar success rates but in significantly smaller amounts of time.
- We implement our approach on a real robotic system and compare it with the standard MPC.

II. PROBLEM DESCRIPTION

We consider the problem where a robot must plan a sequence of non-prehensile actions to take an environment from an initial configuration to a desired goal configuration. We consider two task categories: In the *pushing task* the goal is to push a target object into a goal region; and in the *grasping in clutter* task the goal is to bring a target object, among other objects, into the robot's hand. Our scenes contain D dynamic objects. x^i refers to the full pose (translation and rotation) of each dynamic object, for $i = 1, \dots, D$. We assume a flat working surface with edges and the robot is not allowed to drop objects off the edges.

We consider a 6 degrees of freedom manipulator with a 1-DOF end-effector (gripper) constrained to move in the same plane as our working surface. The robot's configuration is defined by a vector of joint values $x^R = (\theta_x, \theta_y, \theta_{rotation}, \theta_{gripper})$. We represent the complete state of our system as x_t at time t . This includes the configuration and velocity of the robot and all dynamic objects; $x_t = (x^R, x^1, \dots, x^D, \dot{x}^R, \dot{x}^1, \dots, \dot{x}^D)$.

The controls in our case are velocities applied to the robot's end-effector in the plane: $u_t = (\dot{\theta}_x, \dot{\theta}_y, \dot{\theta}_{rotation}, \dot{\theta}_{gripper})$. These velocities are transformed through the Jacobian and then applied to the manipulator's degrees of freedom. We then

define the stochastic discrete time dynamics of our system as:

$$x_{t+1} = f(x_t, u_t) + \zeta(x_t, u_t) \quad (1)$$

where f is the stochastic state transition function that describes the evolution of state x_t given the action u_t , and ζ is the plant dynamics noise. We assume an initial state of the system x_0 . Our goal is to generate a sequence of actions for the robot such that the desired final goal configuration of the environment is reached as quickly as possible without dropping objects off the edge of our working surface. In the foregoing paragraphs, $u_{0:n-1}$ denotes a sequence of control signals of fixed duration Δ_t applied in n time steps. In the same vein, we represent a sequence of states as $x_{0:n}$. Our state transition function is modelled with a physics engine [14]. Physics engines are an inaccurate model of the real world especially in domains with contact. Moreover, it is difficult for the robot to have complete knowledge of the geometric, inertial and frictional properties of the environment. Our aim is to generate actions that succeed even under model inaccuracies of the system and its dynamics.

III. FORMULATION AS A MARKOV DECISION PROCESS

To build a task-adaptive controller, we formulate our problem as an MDP, and we provide an approximate solution to it. An MDP is defined by a tuple $\langle S, U, P, L \rangle$, where S is the set of states, U is the set of actions, P is the probabilistic transition function, and L defines the costs. In our problem S is given by all possible values of x_t as described in the previous section. Similarly, U is given by all possible values of u_t , and P can be computed using the stochastic relation in Eq. 1. The cost function L at every step is:

$$l(x_t, x_{t+1}, u_t) = \sum_i^D w_e \cdot e^{k \cdot d_p^i} + w_s \cdot (x_{t+1}^i - x_t^i)^2 + k_{act} \quad (2)$$

The first term in the cost penalizes a pushed object if it gets too close to or leaves the table's boundaries. We show the edge cost in Fig. 4 where we define a safe zone smaller than the table's boundaries. If an object is pushed out of this safe region as a result of a single action between t and $t+1$, we compute the pushed distance d_p . Also note that k is a constant term and no edge costs are computed for objects in the safe zone. The second term in the cost penalizes if dynamic objects are moved away from their current locations. The third term, k_{act} is a constant cost incurred for each action taken by the robot. w_e and w_s are weights for the edge and state deviation costs respectively.

The optimal policy for a discrete MDP is given by:

$$\pi^*(x) = \arg \min_{u \in U} \left[l(x, u) + \gamma \cdot \sum_{x' \in S} P(x'|x, u) \cdot V^*(x') \right] \quad (3)$$

where $0 < \gamma < 1$ is the discount factor, and V^* is the optimal value function.

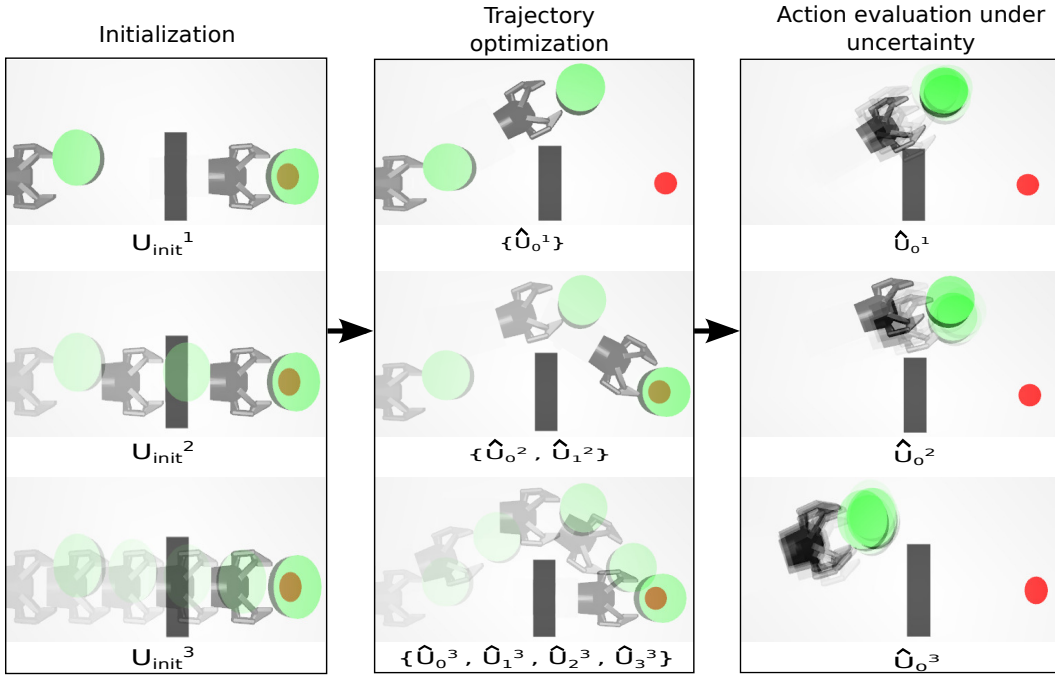


Fig. 2: First column: Initialization of our task-adaptive approach with control sequences including fast (top) and slow (bottom) actions. Second column: Stochastic trajectory optimization of the initial candidate control sequences. Last column: Action evaluation under uncertainty through sampling.

An online one-step lookahead approximate solution to the MDP problem can be found by sampling and evaluating the average value over samples as in Péret and Garcia [12]:

$$\tilde{\pi}(x) = \arg \min_{u \in U} \left[l(x, u) + \frac{1}{Q} \cdot \sum_{x' \in S(x, u, Q)} \tilde{V}(x') \right] \quad (4)$$

where $S(x, u, Q)$ is the set of Q samples found by stochastically propagating (x, u) , and \tilde{V} is an approximation of the value function.

This solution requires propagating Q samples for every possible discretized action u , to find the one with the minimum cost. Performing this for all actions $u \in U$ is not feasible for our purposes for a variety of reasons: First, we are interested in actions that span a wide range of speed profiles (i.e. fast and slow), which make our potential action set large; second, each propagation in our domain is a physics simulation which is computationally expensive; and third, our goal is closed-loop pushing behavior close to real-time speeds.

We present our algorithm for the online MDP approximate solution in Alg. 1. Instead of using a large action set, we propose to use a small set of promising actions with a variety of speed profiles. We identify such a set of actions using a trajectory optimizer based on the deterministic dynamics function f of the system.

We begin by generating U_{init} which contains N straight line velocity profiles to the goal. These N profiles contain control sequences with different numbers of actions of fixed duration Δ_t . On line 2 of the algorithm, the procedure *GetActionSet* returns a restricted set of action sequences from which we

get the first actions in line 3. We explain the details of how this action selection is performed in Sec. IV. In the algorithm, between lines 4-10, we compute the value of each action via sampling. Between lines 6-9, we calculate the value of one sample. On line 7, we perform a stochastic execution of our model of the system dynamics. More specifically, we apply the controls (velocities) to the robot for the duration Δ_t and thereafter we wait for a fixed extra time (t_{rest}) for the objects to come to rest before computing the cost. We use a physics engine to model the dynamics and induce stochasticity by adding Gaussian noise on the velocities $v_{\Delta_{t_{sim}}}$ of the robot and objects at every simulation time step $\Delta_{t_{sim}}$:

This approach is summarized in Fig. 2 where we have an example scene with a planar gripper and a green goal object. The task is to push the goal object to a desired goal location (the red spot) while avoiding the rectangular black region. Our method begins with generating straight line action sequences ($N = 3$) to the goal as shown in the first column with fast and slow actions since each action is of fixed duration. The next step then is to optimize these trajectories such that the robot pushes the target object to the goal location and also avoids obstacles. Afterwards, we take the first action from each of the optimized control sequences and evaluate them under uncertainty through sampling. Thereafter, we calculate the average cost of the various actions, we pick the best one and execute it. Moreover, at the next iteration, in addition to generating new straight line control sequences to the goal, we also re-use the best control sequence from the previous iteration. This process is then repeated until task completion.

$$\tilde{v}_{\Delta_{tsim}}^i = v_{\Delta_{tsim}}^i + \mu^i, \quad \mu^i \sim \mathcal{N}(0, \beta^i) \quad (5)$$

where \mathcal{N} is the Gaussian distribution and β^i is the variance for object i . On line 8, we calculate the cost using Eq. 2. On line 9, C^u is the utility/approximate value function \hat{V} of the next state which is returned by the *GetActionSet* procedure in line 2 for each action.

Algorithm 1: Online MDP solver

Input : x : Initial state
 $U_{init} \leftarrow N$ straight line profiles to the goal

Parameters : Q : Number of stochastic samples
 N : Desired number of action sequences

```

1 while task not complete do
2    $\hat{U}, C \leftarrow \text{GetActionSet}(x, U_{init})$ 
3    $\hat{U}_0 \leftarrow \{\hat{U}_0^1, \hat{U}_0^2, \dots, \hat{U}_0^N\}$   $\triangleright$  Get the first actions
4   for each  $u$  in  $\hat{U}_0$  do
5      $V^u = 0$ 
6     for  $i \leftarrow 0$  to  $Q - 1$  do
7        $x^{u,i} = \text{ExecuteStoch}(x, u)$ 
8        $V^{u,i} = \text{CalculateCost}(x, x^{u,i}, u)$ 
9        $V^u = V^u + V^{u,i} + C^u$ 
10     $V^u = V^u / Q$ 
11     $\tilde{u} = \arg \min_{u \in \hat{U}} V^u$ 
12     $x \leftarrow \text{execute } \tilde{u}$ 
13    check task completion
14     $U_{init} \leftarrow \hat{U}_1$   $\triangleright$  Update  $U_{init}$ 
```

IV. GENERATING A VARIETY OF ACTIONS

Our task here is to generate a good set of actions that will be sent to our online MDP solver. We use sampling-based trajectory optimization as a planner that quickly suggests candidate actions. We explain our sampling-based algorithm in Sec. IV-B. Moreover, the sampling based algorithm, requires initialization and we exploit this to force the trajectory optimizer to return a variety of actions. More specifically, we initialize the trajectory optimizer with trajectories of varying time horizons and number of actions as shown in Alg. 2.

Algorithm 2: Generating a set of actions

Input : x_0 : Initial state
 U_{init} : Set of N action sequences

Output : \hat{U} : Optimized set of action sequences
 C : Cost set of each of the N action sequences starting from the second action

```

1 for  $k \leftarrow 0$  to  $N - 1$  do
2    $\hat{U}^k, C_k \leftarrow \text{STO}(x_0, U_{init}^k)$ 
3 return  $(\hat{U}, C)$ 
```

In Alg 2, we use each profile U_{init}^k to initialize *STO* such that it finds a locally optimal solution (lines 2-3). We then return the N optimal control sequences \hat{U} , and the cost set



Fig. 3: Goal cost terms

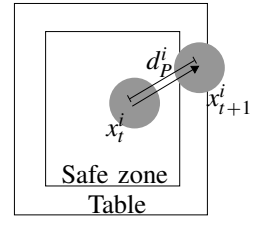


Fig. 4: Edge cost terms

C for each action sequence starting from the second action. More specifically, C represents the approximate value function for the next state used in our online MDP solver after we stochastically evaluate the first action.

A. Finite Horizon Optimal Control

In finite horizon optimal control, we define a planning horizon, n and a cost function J as:

$$J(x, u_{0:n-1}) = \sum_{t=0}^{n-1} l(x_t, u_t) + l_f(x_n) \quad (6)$$

J is obtained by applying the control sequence $u_{0:n-1}$ starting from a given initial state and includes the sum of running costs l and a final cost l_f . Note that x_t must satisfy the state transition function constraint $x_{t+1} = f(x_t, u_t)$. Then the optimal solution is the minimizing control sequence:

$$u_{0:n-1}^* = \arg \min_{u_{0:n-1}} J(x, u_{0:n-1}) \quad (7)$$

B. Stochastic Trajectory Optimization

With parallel rollouts on multiple cores of a PC, recent stochastic trajectory optimization methods such as STOMP [7] and model predictive control methods such as MPPI [15] show impressive speed. In addition, these stochastic optimization methods can use arbitrary cost functions that do not have to be differentiable. In contrast with sampling-based methods such as RRTs and PRMs [8, 11], optimization approaches are able to produce lower cost trajectories within a time limit even if they do not take the system to the desired goal state. These benefits make stochastic trajectory optimization very attractive. In this work, we propose Alg. 3 which adapts the STOMP algorithm [7] for non-prehensile object manipulation.

We begin with an initial nominal control sequence $u_{0:n-1}$ and iteratively seek lower cost trajectories (lines 2-12) until the cost reaches a threshold or until the maximum number of iterations is reached (line 2). We add stochastic noise on the nominal control sequence to generate K new control sequences at each iteration (line 5), we then propagate the states and compute the costs along the trajectory for each of the K samples (lines 3 - 7). Thereafter, we pick the minimum cost trajectory and set it as the new nominal control sequence for the next iteration.

The cost terms for the state-action sequences in this algorithm are equal to the running costs in Eq. 2, with the addition of a terminal cost on the final state depending on the task. The

Algorithm 3: Stoch. Traj. Optim. (STO)

Input : x_0 : Initial state
 $u_{0:n-1}$: Initial control sequence
Output : $u_{0:n-1}$: Optimal control sequence
Parameters : K : Number of noisy trajectory rollouts
 v : Sampling variance
 C_{thresh} : Success definition in terms of cost
 I_{max} : Maximum number of iterations
Subroutines: *Cost*: Computes total cost, i.e. Eq. 6

```

1  $x_{0:n} \leftarrow$  Roll out  $u_{0:n-1}$  over  $x_0$  to get initial state sequence
2 while  $I_{max}$  not reached and  $Cost(u_{0:n-1}, x_{0:n}) > C_{thresh}$  do
3   for  $k \leftarrow 0$  to  $K - 1$  do
4      $x_0^k \leftarrow x_0$ 
5      $u_{0:n-1}^k \leftarrow N(u_{0:n-1}, v)$ 
6     for  $t \leftarrow 0$  to  $n - 1$  do
7        $x_{t+1}^k \leftarrow f(x_t^k, u_t^k)$ 
8      $k^* \leftarrow \arg \min_k (Cost(u_{0:n-1}^k, x_{0:n}^k))$ 
9     if  $Cost(u_{0:n-1}^{k^*}, x_{0:n}^{k^*}) < Cost(u_{0:n-1}, x_{0:n})$  then
10       $u_{0:n-1} \leftarrow u_{0:n-1}^{k^*}$ 
11       $x_{0:n} \leftarrow x_{0:n}^{k^*}$ 
12 return  $(u_{0:n-1}, x_{0:n}), Cost(u_{0:n-1}^{k^*}, x_{0:n}^{k^*})$ 

```

terminal cost for the pushing task is given by:

$$l_f = \begin{cases} 0 & \text{if } R_o - R_g < 0 \\ w(R_o - R_g)^2 & \text{if } R_o - R_g > 0 \end{cases}$$

where w is a constant, R_o is the distance between the pushed object and the center of a circular goal region of radius R_g .

The terminal cost term for the task of grasping in clutter is given by: $d_T^2 + w_\phi \cdot \phi_T^2$. We show how the distance d_T and the angle ϕ_T are computed in Fig. 3. First, create a vector from a fixed point in the gripper to the target object where d_T is the length of this vector and ϕ_T is the angle between the forward direction of the gripper and the vector. We use w_ϕ to weight angles relative to distances.

V. BASELINE APPROACH

In this paper, we implement a standard model predictive control algorithm (*SMPC*) as a baseline approach. It involves repeatedly solving a finite horizon optimal control problem using the stochastic trajectory optimizer presented in Alg. 3 and proceeds as follows: optimize a finite horizon control sequence, execute the first action, get the resulting state of the environment and then re-optimize to find a new control sequence. When re-optimizing, we warm-start the optimization with the remaining portion of the control sequence from the previous iteration such that optimization now becomes faster. In addition, we propose another baseline approach to compare against in this work: uncertainty aware model predictive control (*UAMPC*). This is a version of our online MDP solver where only low speed actions are considered.

VI. EXPERIMENTS

We verify how well our approach is able to handle uncertainty and adapt to varying tasks. First, we compare the performance of our task-adaptive online trajectory optimization (*TAMPC*) approach with a standard model predictive control method (*SMPC*). Here we hypothesize that:

- *TAMPC* will complete a given pushing task within a significantly shorter period of time.
- *TAMPC* will be able to adapt to different tasks, maintaining a high success rate under varying levels of uncertainty.
- With a limited time budget, *SMPC* will not be able to maintain a high success rate for high accuracy tasks.

Next, we compare the performance of our approach with uncertainty aware MPC (*UAMPC*). Here we hypothesize that:

- *UAMPC* will have a similar success rate in comparison with *TAMPC*
- *UAMPC* will take a longer amount of time to complete the task in comparison with *TAMPC*

Furthermore, we investigate whether using our algorithm, a robot can exhibit a truly task-adaptive behaviour in different environments: executing fast dynamic pushes for tasks where a low level of accuracy is required and executing slow quasi-static pushes for high accuracy tasks. We implemented our algorithms in Python using the Mujoco [14] physics engine. We conduct experiments in simulation and on a real robotic system for push planning and grasping an object in clutter. Given an environment for planning, we create two instantiations of it:

Planning environment: The robot generates plans in the simulated planning environment. The trajectory optimizer (Alg. 3) uses deterministic physics during planning and our online MDP solver uses stochastic physics as dictated by Eq. 1 to evaluate actions.

Execution environment: Here, the robot executes actions and observes the state evolution. The execution environment is stochastic. It is the physical world for real robot experiments but it is simulated for simulation experiments. In our simulation experiments, uncertainty level refers to the degree of stochasticity which is dictated by the variance of the Gaussian noise β injected at every simulation time step in Eq. 5.

A. Push planning simulation experiments

We present a high accuracy task in Fig. 5e which is a very thin strip with a small goal region. We also define a low accuracy task in Fig. 5a which is a much larger table with a wider goal region. We create 200 such planning environments for each of the high and low accuracy tasks. For each environment:

- We randomly select the shape (box or cylinder) of the pushed object.
- For each goal object, we randomly select¹ shape dimensions (radius and height for the cylinder, extents for the

¹ The uniform range used for each parameter is given here. Box x-y extents: [0.05m, 0.075m]; box height: [0.036m, 0.05m]; cylinder radius: [0.04m, 0.07m]; cylinder height: [0.04m, 0.05m]; mass: [0.2kg, 0.8kg]; coef. fric.: [0.2, 0.6].

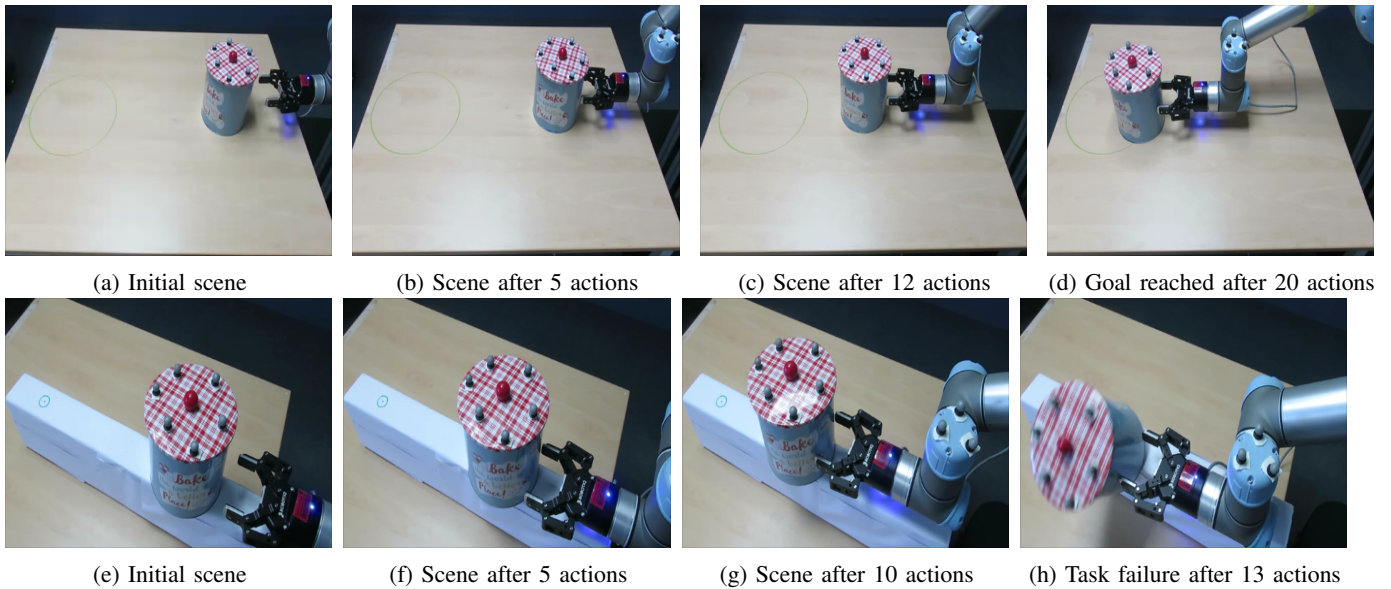


Fig. 5: *SMPC* using a large number of actions to successfully complete a low accuracy level task (a-d), and causing the pushed object to fall off the edge for a high accuracy level task (e-h).

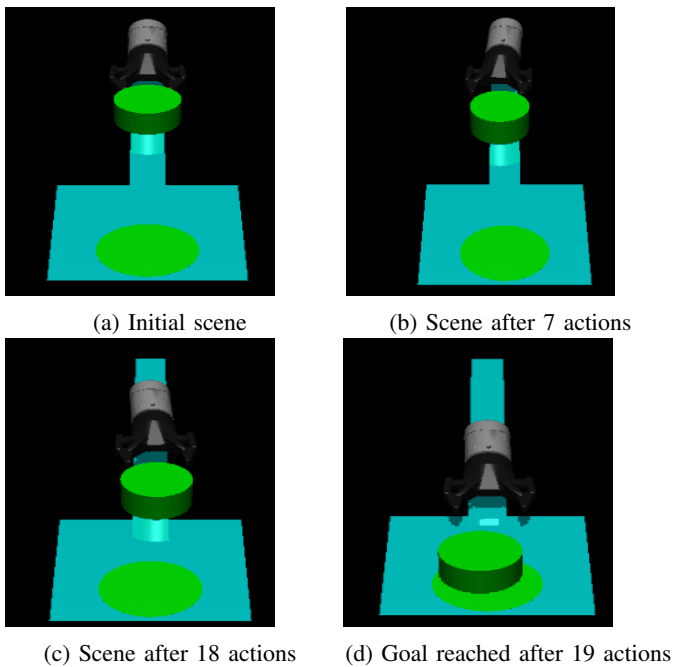


Fig. 6: Push planning in a changing environment with slow pushes initially (a-c) due to the narrow strip and a single final action (d) that completes the task.

boxes), mass, and coefficient of friction.

- We randomly² select a position on the working surface for the pushed object.

² The random position for the pushed object is sampled from a Gaussian with a mean at the lower end of the table ($0.1m$ from the edge of a $0.6m$ long table along the center axis and a variance of $0.01m$).

The concept of uncertainty level is dictated by the variance of the Gaussian noise injected at every simulation time step. We create four uncertainty levels: no uncertainty, low uncertainty, medium uncertainty and high uncertainty. For the no uncertainty case, no extra noise was added to the physics engine. For low, medium and high levels of uncertainty, $\beta^i = \{0.003, 0.006, 0.009\}$ respectively. We test different *MPC* algorithms and specify a timeout of 3 minutes including all planning, re-planning and execution for each of the algorithms. We use only the edge cost term as the running cost during push planning.

Success rates: We declare success when the robot is able to push the goal object to the target region without dropping it off the edge of the table within the specified time limit. We plot the results in Fig. 7a and Fig. 7c. For the low accuracy level push planning task (Fig. 7a), *TAMPC* and *UAMPC* were able to maintain a 100 % success rate while *SMPC* showed a slight decrease in success rates as uncertainty grew. For the high accuracy pushing task (Fig. 7c), *TAMPC* and *UAMPC* were also able to maintain a good average success rate. However, *SMPC* fails to adapt yielding a poor performance as the uncertainty grew.

Furthermore, recall that *SMPC* involves planning a set of actions to be applied on the robot sequentially one after the other for a fixed time horizon, the first action is applied and the process is repeated. The policy-lag (re-planning time) is high in this domain, typically requiring the robot to execute an action, stop and wait until the next action becomes available. If an action injects acceleration on a pushed object, it will continue moving after the robot has stopped to re-plan. Then, undesired events such as objects falling off the table can occur solely due to the policy-lag with *SMPC*. We address this

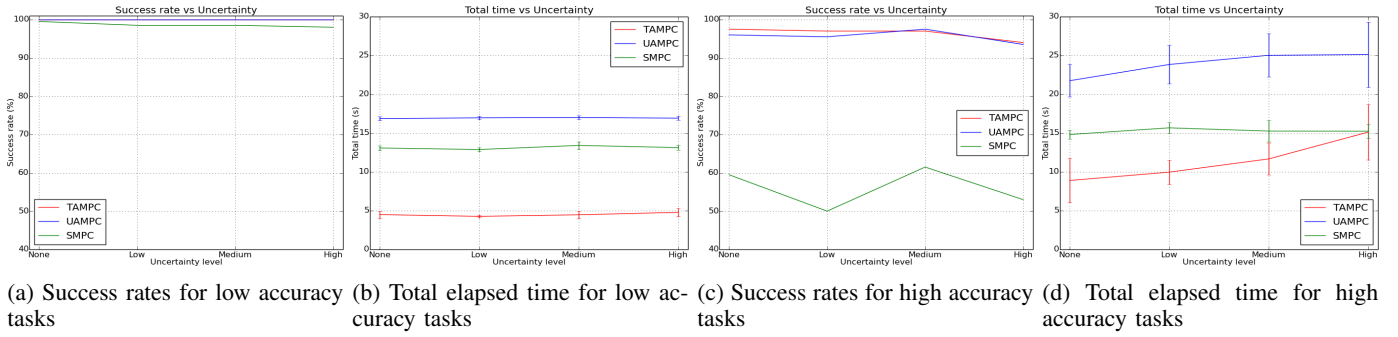


Fig. 7: Success rate and total elapsed time versus uncertainty level for low accuracy tasks (a-b). Success rate and total elapsed time versus uncertainty level for high accuracy tasks (c-d).

problem in *TAMPC* (Sec. III) during planning by waiting for objects to come to rest before computing the cost of an action.

Total time: The total time in our experiments includes all planning and execution time. Fig 7b and Fig 7d show the average of 200 scenes with 95 % confidence interval of the mean. For the low accuracy level task, our *TAMPC* planner is able to achieve the goal in under 5s (Fig 7b), while *UAMPC* and *SMPC* took significantly more time to complete the task. This clearly shows that our method is able to generate successful fast actions while maintaining a high success rate. For the high accuracy level task (Fig 7d), our planner is able to generate as many small actions as needed as the uncertainty grew. Hence it was able to maintain a high success rate and still complete the task within a very small amount of time in comparison with the baseline approach.

Furthermore, we investigate the adaptive behaviour of our approach for a changing environment in Fig. 6d. Where the robot executes small pushes while on the thin strip but realises at the end of the strip that a single dynamic push is able to complete the task.

B. Grasping in clutter simulation experiments

We conducted a small number of simulation experiments for grasping in clutter. Our scenes contain 15 randomly generated objects (boxes and cylinders) and a robot with four control inputs (including the gripper). We tested our task adaptive planner in clutter to observe how the planner adapts given different environment configurations. We see that the robot manipulates clutter and is able to grasp the target object. An example scene is shown in Fig. 8. For a difficult grasping in clutter problem (Fig. 8(a-d)), the robot is able to select small action sizes and plan locally optimal actions that push objects aside until it grasps the target object. However, for the less difficult task (Fig. 8(e-f)), the robot is able to complete the task with a single action. We include the state deviation cost term during grasping in clutter.

C. Real robot experiments

In the real robot experiments we use a UR5 robot with a Robotiq 2 finger gripper attached as the end effector. We restrict the motion of the gripper to a plane parallel to the working surface such that we have a planar robot. We use OpenRave

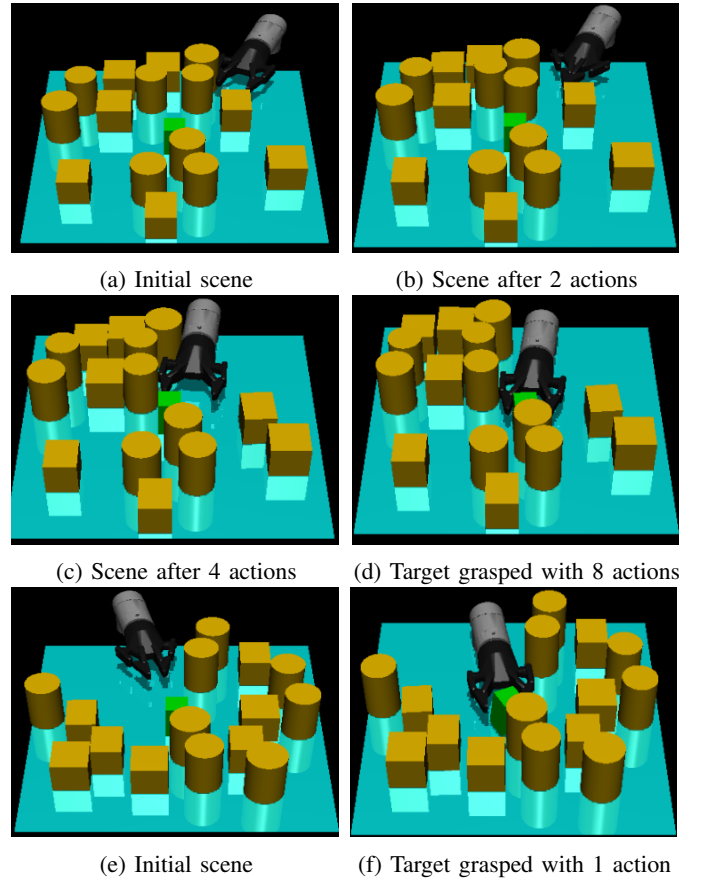


Fig. 8: Grasping in clutter for a critical task (a-d) where the robot pushes on obstacles and successfully clears a path to the goal object. However, for a less critical task (a-f), the robot grasps the target object with a single action.

[2] to find kinematics solutions at every time step. For the push planning experiments, the gripper is completely open such that the robot receives 3 control inputs $u_t = (\theta_x, \theta_y, \theta_{rotation})$ at every time step. We use a medium uncertainty level to model the real world stochasticity. We place markers on the pushed object and track its full pose with a motion capture system [13]. We manually replicated 3 execution worlds for each

task accuracy level from the randomly generated environments we created during push planning simulation experiments. We tested our planners in these environments. We show snapshots from our real robot experiments. In Fig. 5a, we have a low task accuracy environment where the standard MPC approach is successful after 20 actions. However, by using a single dynamic push in Fig. 1, our task-adaptive control approach is able to complete the push planning task in under 2 seconds.

Moreover, for the high task accuracy problem, *SMPC* was unable to push the target object to the desired goal location (Fig. 5e). It executes actions without reasoning about uncertainty and pushed the goal object off the edge. Our task-adaptive controller was able to generate small pushes (Fig. 1) to complete the task with 21 actions. These results can be found in the accompanying video at <https://youtu.be/g7qMEzVcAjA>

VII. CONCLUSION

In this work, we have presented a task-adaptive model predictive controller capable of adapting to the accuracy requirements of a task by generating both fast and slow actions. Robots today are driven with very conservative actions most of the time, but this could change if a task adaptive system were put in place. In the future, we will investigate the generalization of this task-adaptive system to other manipulation primitives and show its performance in more difficult tasks.

REFERENCES

- [1] Ermano Arruda, Michael J. Mathew, Marek Sewer Kopicki, Michael Mistry, Morteza Azad, and Jeremy L. Wyatt. Uncertainty averse pushing with model predictive path integral control. *CoRR*. URL <http://arxiv.org/abs/1710.04005>.
- [2] R. Diankov, S. S. Srinivasa, D. Ferguson, and J. Kuffner. Manipulation planning with caging grasps. In *Humanoids 2008 - 8th IEEE-RAS International Conference on Humanoid Robots*, pages 285–292, Dec 2008. doi: 10.1109/ICHR.2008.4755966.
- [3] Mehmet R Dogar, Kaijen Hsiao, Matei Ciocarlie, and Siddhartha Srinivasa. Physics-based grasp planning through clutter. In *Robotics: Science and Systems*, 2012.
- [4] Francois Robert Hogan and Alberto Rodriguez. Feedback control of the pusher-slider system: A story of hybrid and underactuated contact dynamics. *CoRR*, abs/1611.08268, 2016. URL <http://arxiv.org/abs/1611.08268>.
- [5] Robert D Howe and Mark R Cutkosky. Practical force-motion models for sliding manipulation. *The International Journal of Robotics Research*, 15(6):557–572, 1996.
- [6] Aaron M. Johnson, Jennifer King, and Siddhartha Srinivasa. Convergent planning. 1(2):1044–1051, July 2016.
- [7] Mrinal Kalakrishnan, Sachin Chitta, Evangelos Theodorou, Peter Pastor, and Stefan Schaal. Stomp: Stochastic trajectory optimization for motion planning. In *Robotics and Automation (ICRA), 2011 IEEE International Conference on*, pages 4569–4574. IEEE, 2011.
- [8] Jennifer E King, Joshua A Haustein, Siddhartha S Srinivasa, and Tamim Asfour. Nonprehensile whole arm rearrangement planning on physics manifolds. In *Robotics and Automation (ICRA), 2015 IEEE International Conference on*, pages 2508–2515. IEEE, 2015.
- [9] N. Kitaev, I. Mordatch, S. Patil, and P. Abbeel. Physics-based trajectory optimization for grasping in cluttered environments. In *2015 IEEE International Conference on Robotics and Automation (ICRA)*, pages 3102–3109, May 2015.
- [10] Matthew T. Mason. Mechanics and planning of manipulator pushing operations. *The International Journal of Robotics Research*, 5(3):53–71, 1986. doi: 10.1177/027836498600500303.
- [11] Muhayyuddin, M. Moll, L. Kavraki, and J. Rosell. Randomized Physics-based Motion Planning for Grasping in Cluttered and Uncertain Environments. *ArXiv e-prints*, November 2017.
- [12] Laurent Péret and Frédéric Garcia. On-line search for solving markov decision processes via heuristic sampling. In *Proceedings of the 16th European Conference on Artificial Intelligence*, pages 530–534. IOS Press, 2004.
- [13] OptiTrack Motion Capture Systems. URL <https://optitrack.com/>.
- [14] Emanuel Todorov, Tom Erez, and Yuval Tassa. Mujoco: A physics engine for model-based control. In *Intelligent Robots and Systems (IROS), 2012 IEEE/RSJ International Conference on*, pages 5026–5033. IEEE, 2012.
- [15] Grady Williams, Andrew Aldrich, and Evangelos Theodorou. Model predictive path integral control using covariance variable importance sampling. *CoRR*. URL <http://arxiv.org/abs/1509.01149>.